Assessment of Upper-Body Movement Quality in the Cartesian-Space is Feasible in the Harmony Exoskeleton

Ana C. De Oliveira and Ashish D. Deshpande

Abstract—To determine the most effective interventions for poststroke patients, it is imperative to monitor the recovery process. Robotic exoskeletons' built-in sensing capabilities enable accurate kinematic measurement with no additional setup time. Although position sensors used in exoskeletons are accurate, a mismatch between the robot's and the human's joints can lead to inaccurate measurements. In addition, the robot's residual dynamics can interfere with human's natural movements and the kinematic metrics assessed in the robot would not be representative of the human's movement in free-motion. So far, the accuracy of robotic exoskeletons in assessing upper-body kinematics has not been verified. The bilateral upper-body Harmony exoskeleton has features favorable to minimize joint misalignments and the robot's residual dynamics. In this study, we examined Harmony's ability to accurately assess Cartesian-space kinematic parameters associated with the wearer's movement quality. We analyzed data collected from eight healthy participants that executed point-to-point movements with and without the presence of the robot and at fast and slow speeds. Ground truth was acquired with an optical motion capture, and we extracted the kinematic parameters from the measured data. The results suggest that Harmony can accurately measure kinematic parameters associated with movement quality, and these parameters could appropriately reflect wearer's natural movements at a slow speed. Therefore, Harmony could aid the evaluation of the effectiveness of different interventions, which is more sensitive and efficient than currently adopted clinical outcomes. This allows for individualization of a treatment plan and a detailed follow-up.

Index Terms—Kinematic assessment, motion capture, rehabilitation robotics, robotic exoskeleton.

I. INTRODUCTION

VERY year, around 800 000 people suffer a stroke in the United States [1]. Over 80% of stroke survivors suffer

Manuscript received 29 December 2022; revised 13 June 2023; accepted 22 July 2023. Date of current version 14 December 2023. This work was supported in part by CAPES (Brazil), in part by the NSF under Grant 1941260 and Grant 2019704, and in part by Facebook. This article was recommended by Associate Editor J. Yang. (Corresponding author: Ashish D. Deshpande.)

This work involved human subjects or animals in its research. Approval of all ethical and experimental procedures and protocols was granted by the Internal Review Board of the Office of Research Support in The University of Texas at Austin under Application No. 2013-05-0126, and performed in line with the university requirements.

The authors are with the Walker Department of Mechanical Engineering, The University of Texas at Austin, Austin, TX 78712 USA (e-mail: ana.oliveira@utexas.edu; ashish@austin.utexas.edu).

Color versions of one or more figures in this article are available at https://doi.org/10.1109/THMS.2023.3305391.

Digital Object Identifier 10.1109/THMS.2023.3305391

from hemiparesis (weakness of one side of the body). Several motor deficits associated with hemiparesis [2] affect the patient's ability to carry through daily activities with arms and shoulders [3], [4], [5], [6]. Rehabilitation aims to promote the independence of stroke patients [7], but to determine the most effective interventions for each individual, it is imperative to monitor the recovery process [8], [9]. Outcome measures often adopted in conventional practice to assess function [10], [11] and impairment [12] are inherently subjective and highly variable. Assessment of kinematic features associated with movement quality [13], [14] has been increasingly adopted in research settings due to its consistency and higher sensitivity to changes compared to conventional measures [15]. For instance, a study demonstrated that kinematic metrics can distinguish if functional improvements are associated with compensatory strategies or impairment mitigation [16]. Motion capture (mocap) systems are an accurate and reliable sensing modality to capture kinematics. However, they require a controlled environment and a long setup time, being impractical for clinical use. Robotic exoskeletons adopted for upper-body rehabilitation [17], [18], [19], [20] are promising for clinical applications because they can simultaneously deliver training at high dosage and intensity while assessing motor abilities, thanks to their built-in sensing capabilities.

While position sensors are prevalent and accurate in robotic exoskeletons, a mismatch in the center of rotation of the exoskeleton and anatomical joints could lead to inaccurate estimation of body kinematics. So far, the accuracy of robotic exoskeletons in assessing body kinematics has not been verified [21]. Furthermore, the robot's residual dynamics can interfere with a human's natural movements [22], [23], so the kinematic metrics assessed in the robot would not be representative of the human's movement in free motion. High backdrivability can minimize the robot's interference with human's movements, but most of existing robotic exoskeletons [24] are powered via geared motors [25], [26] or cable-driven actuators [27], which have limited backdrivability. Kim and Deshpande [28] have developed the Harmony exoskeleton to address several limitations previously identified in upper-body robotic exoskeletons. It is a high-performance device that can safely accommodate the natural coordination of the shoulder [29] and supports bilateral training. Harmony is actuated with series elastic actuators, which exhibit high-performance in torque control and optimize the robot's backdrivability. Therefore, we can exploit Harmony's

2168-2291 © 2023 IEEE. Personal use is permitted, but republication/redistribution requires IEEE permission. See https://www.ieee.org/publications/rights/index.html for more information.

capabilities to accurately evaluate kinematic parameters in parallel with the rehabilitation training. For quantitative accuracy, the robot's assessment must be equivalent to another reliable method such as mocap. For an accurate qualitative representation of a human's natural and unassisted movement, the robot must not physically interfere with their movement. Since it is unfeasible to fully mitigate the robot's interference in the human's movements, to maximize accuracy, we must determine the conditions that minimize the robot's physical interference to human-driven motion.

In a previous work [30], we compared joint angles measured by Harmony with joint angles simultaneously obtained from mocap measurements. The results demonstrated that Harmony's measurements of distal joints (elbow flexion and forearm pronation) are consistent with mocap's measurements. However, we identified systematic biases between the two sensing modalities in measurements of shoulder plane and angle of elevation, and inconsistencies in measurements of shoulder elevationdepression and protraction-retraction. Results from this study have demonstrated that a properly constrained trunk and a well-adjusted, reasonably rigid interface are two factors that affect the accuracy of joint angles measured by Harmony. Joint angle is an important parameter that can inform clinicians of a patient's range of motion and abnormal coupling between joints. However, several other metrics that are directly associated with movement quality [13] were not investigated in the previous work. In addition to that, we did not evaluate Harmony's interference with the human's natural movements in free motion. In this work, we present a quantitative comparison of kinematic metrics measured by Harmony and an optical mocap system during reaching movements. Our goals are: 1) to investigate whether kinematic metrics of movement quality measured by the robot are equivalent to the ones measured with the current gold standard; and 2) to determine if Harmony can accurately capture the human's natural movement (i.e., in free motion). We adopted four well-established metrics [14] in Cartesian-space frequently used in reaching tasks to assess movement planning, efficiency, smoothness, and speed. These metrics may capture features relevant to stroke recovery, from compensatory movements [14] to motor impairment in specific characteristics of the movement such as smoothness [31] and acceleration patterns [32]. In addition, the chosen metrics may have association with widely adopted assessment methods, such as the Fugl-Meyer (FM) scale [12]. Because movement ability might exhibit directional dependence [33], we performed a direction-specific analysis with targets distributed in the vertical and horizontal planes to allow for investigation in 3-D movements under different gravitational effects. This work may lead to accurate and clinically relevant assessments during poststroke rehabilitation.

II. METHODS

Our goal is to quantitatively compare Cartesian-space kinematic metrics measured by Harmony and an optical mocap system during reaching movements. These metrics are associated with the movement quality of the hand motion and require measurement of the hand-position during the entire assessment

TABLE I STANDARD DENAVIT—HARTENBERG PARAMETERS FOR THE KINEMATIC MODEL OF HARMONY'S RIGHT ARM

Joint	a	α	d	θ
1	L_c	-90°	0	θ_1^*
2	0	0	0	$ heta_2^*$
2′	0	90°	0	$-\theta_{2}^{*} + 18^{\circ}$
3	0	-60°	0	$\theta_3^* = 30.75^{\circ}$
4	0	60°	0	$\theta_4^* + 87.2^{\circ}$
5	L_h	0	0	$\theta_5^* - 112.87^\circ$
6	0	0	0	$\theta_6^* + 90^{\circ}$
6′	0	90°	0	0
7	0	0	L_f	θ_7^*

task. The hand movement can be directly tracked using mocap with markers placed on the hand. Harmony is equipped with position encoders attached axially to each of the robot's actuated joints. To infer hand movement from these encoder readings, we adopted the kinematic model defined by the Denavit–Hartenberg parameters [34] presented in Table I. This model represents Harmony's kinematic chain with nine DOFs: seven actuated joints, one passive joint to accommodate the 4-bar-mechanism structure of the shoulder, and one passive joint to adjust the end-point frame. Symbols θ_i^* represent the angle measured in the actuated joint i. The quantities represented by L_c , L_h , and L_f are the known lengths of the clavicle, humerus, and forearm, respectively. The hand position can be inferred from the end-effector frame.

A. Experimental Protocol

We carried out an experiment with able-bodied individuals, where participants performed a series of 3-D reaching movements with their right arm going from the initial position toward a target (outbound) and back to the initial position (inbound). We defined nine targets distributed in two semicircles of the same radius. The semicircles, each containing five targets, were centered at the initial position, oriented parallel to the sagittal and transverse planes, and intercepting in the middle, as shown in Figs. 1(b) and 2. To determine the location of the targets, we defined the useful workspace length (Ω) , which is given by a participant's arm length (L_a) subtracted by the estimated position of a human's useful workspace boundary, defined as 20 cm from the glenohumeral joint. The target distribution was adjusted such that the initial position was aligned with the participant's right glenohumeral joint in the medial-lateral and superior–inferior directions and located at 0.5 Ω . The radius of the semicircles was set to 40% of Ω . This distribution was chosen to ensure that all targets would be in the field of view at all times and that all targets would be at a reachable yet far enough distance to require significant arm movement.

Participants performed the movements at two different speeds comparable with velocities performed in activities of daily living [35], [36], referred as slow and fast speeds, defined as 15 and 40 cm/s, respectively. They received visual feedback of their current hand position and targets at all times in 3-D space in an immersive virtual reality environment (Oculus VR, Menlo Park, CA, USA). Participants were instructed to move as fast as possible in the fast speed once cued so that they

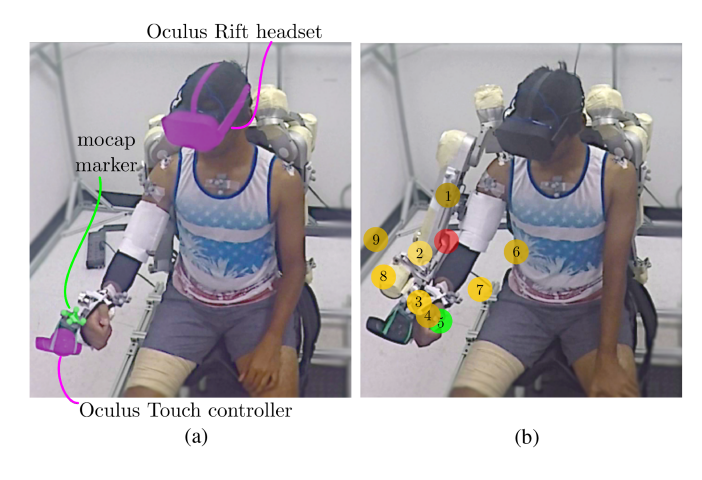


Fig. 1. Experimental setup, where free-motion condition is shown in (a) and in-robot condition is shown in (b). Markers are highlighted in green and Oculus headset and controller are highlighted in pink in (a). The target distribution as seen by the participant is shown in (b), where home position is depicted in red, targets are depicted in yellow, and active target reached by the participant is depicted in green.

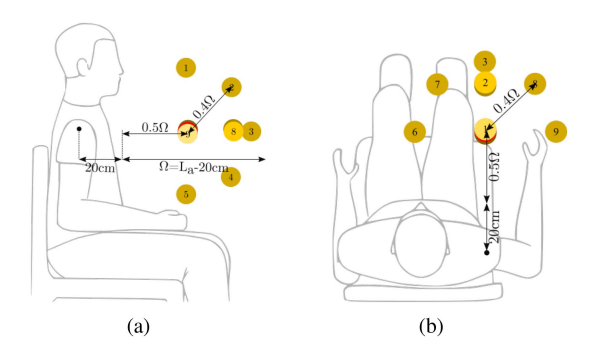


Fig. 2. Targets distribution with respect to a participant's location, where home position is depicted in red and targets are depicted in yellow. The nine targets are numbered as shown as a reference for the analysis. Views parallel to sagittal and transverse planes are shown in (a) and (b), respectively. The quantity Ω represents the useful workspace length, given by the arm length (L_a) subtracted by $20~\rm cm$.

would rely more heavily in their proprioception to achieve a movement speed closer to the intended one because the reaction time to the feedback could slow down the movement significantly. Home position and target distribution were defined in this virtual environment using the inertial frame of the robot, fixed across participants, and the participant's arm lengths as guiding parameters. The experimental setup was the same as described in our previous study [30], where we used the Oculus Touch Controller (Oculus VR, Menlo Park, CA, USA) fixed to the human–robot physical interface as shown in Fig. 1(a) to provide visual feedback of the hand location.

We controlled movement speed using visual and auditory cues. The visual cue consisted of a shrinking sphere surrounding the target and the auditory cue consisted of beeps from a metronome, both programmed to follow the desired speed. Participants were instructed to initiate movement toward the target as soon as they were cued to start. They were asked to control their speed following the pace of beeps to reach the target at the same time as the shrinking sphere reaches

Sensing modality:					Sensing modality:					
MOCAP					MOCAP, ROBOT					
SLOW	FAST	SLOW	FAST		SLOW	FAST	SLOW	FAST		
2x 9 targets	2x 9 targets	2x 9 targets	2x 9 targets		2x 9 targets	2x 9 targets	2x 9 targets	2x 9 targets		
				J					J	
FREE-MOTION					IN-ROBOT					

Fig. 3. Order of experimental conditions in the protocol, showing the two phases with four blocks in free motion and four blocks in in-robot condition. Each phase consisted of alternated blocks, two in slow and two in fast speed, and each block contained two instances of each of the nine targets.

the target's standard size. Prior to the experiment, participants practiced the task outside of the robot to get familiarized with movement speed and range. They reached once to each target in sequential order from target one to nine at both speeds. The experimental protocol included two performance conditions: One where a participant is outside of the robot, referred as "free motion," and another where a participant is wearing Harmony exoskeleton in transparent mode, referred as "in-robot." The transparent mode is achieved with a baseline controller that provides compensation torques for the robot's own weight and friction, and scapulohumeral rhythm support [29]. Due to Harmony's high-performance torque-controlled actuators, the compensation torques elicit low-impedance dynamics, resulting in high-backdrivability with external torques effortlessly applied by the human [28]. Harmony's interfaces are easily detachable from the robot and were kept attached to a participant's arm during the entire experiment to maximize consistency across conditions. The hand interface requires a specific hand placement to grip the hand thenar and hypothenar eminences along with the wrist [37], reducing placement variability across participants.

Participants performed four blocks in each condition, two at a fast speed and two at a slow speed in alternate order, as shown in Fig. 3. The experiment started in the free-motion condition followed by another set in the in-robot condition. Participants rested for 1 min between blocks and 5 min between conditions. Each block contained two instances of each target in random order to minimize learning effects over practice and make performance as homogeneous as possible. The order in each particular block was fixed across participants.

B. Participants

The experimental procedure performed in this study as well as the procedure followed in our previous work [30] were part of the same protocol approved by the Internal Review Board organized by the Office of Research Support in The University of Texas at Austin (protocol number 2013-05-0126 approved on July 18, 2019). We enrolled nine right-handed able-bodied individuals that had no known shoulder injury and body dimensions within the limits of the Harmony exoskeleton (6 Male/3 Female, ages 27.8 ± 5.9 [20, 39] years, clavicle length 20.3 ± 1 [18.5, 21.5] cm, upper-arm length 31.7 ± 0.8 [30, 33] cm, and forearm length 26.3 ± 1.63 [24, 28.5] cm). One of the participants was unable to successfully complete the task, failing to reach the indicated target or to follow the reference velocity in most of the trials, and was excluded from the analysis. Participants provided written informed consent that was reviewed by the Internal Review Board.

C. Data Acquisition and Analysis

We adopted the optical mocap system Optitrack Prime 17W system (NaturalPoint Inc., Corvallis, OR, USA) with passive markers as the benchmark sensing modality for comparison. We used 10 cameras adjusted to overcome constraints and limitations of the environment. Hand position and orientation are directly tracked with markers attached to the back of the physical human-robot interface on the hand, as shown in Fig. 1(a). We tracked mocap data with a sampling rate of 120 fps. Upon manual inspection, we verified that there were no missing markers for more than a few milliseconds, and we performed interpolation using cubic spline followed by a pattern-based interpolation algorithm as necessary. We tracked robot joint angles with built-in high-resolution magnetic rotary encoders (Contelec AG Inc.) with a sampling rate of 100 Hz. We used a tape measure to determine each participant's body dimensions. We used a fourth-order low-pass Butterworth filter with cut-off frequency of 10 Hz to filter both mocap and robot data. We downsampled mocap time-series data to 100 Hz to obtain a common samplingrate between the two sensing modalities and we synchronized the data using the cross-correlation analysis. Furthermore, we defined a minimum velocity threshold to determine the initial time instant and duration of each reaching movement using mocap data.

D. Outcome Measures

Several metrics have been reported in the literature, and the most adopted constructs for evaluating 3-D point-to-point tasks are spatial posture, efficiency, speed, smoothness, and movement planning [14]. In this study, we adopted four established metrics traditionally used in the literature [13], [14], [21] to represent the efficiency, speed, smoothness, and movement planning constructs: 1) path length ratio (PLR); 2) peak speed (PS); 3) spectral arc length (SAL); and 4) time to PS (TPS), respectively. The efficiency measured by the PLR (PLR-efficiency) is given by the ratio between the length of the actual path traveled by the hand and the length of the straight line joining initial and final hand positions [38]. The minimal value of the PLR-efficiency is one, which indicates a perfectly straight path. Schwarz et al. [14] have suggested that PLR-efficiency might be appropriate to capture compensatory movements. The speed measured by PS (PS-speed) is given by the highest instantaneous velocity during the reaching movement [39]. The PS-speed is linearly related to force generation and level of automaticity [32] and a significant association between the PS-speed and the FM Scale [12] has been reported [40]. The smoothness measured by the SAL (SAL-smoothness) is a dimensionless representation of movement smoothness given by the length of the Fourier magnitude spectrum of a segmented velocity profile [31]. Quantities for able-bodied individuals are generally in the [-2, -1]range and, for individuals with motor impairments, it can exceed -5. We used the Matlab code provided by Balasubramanian et al. [31] to calculate SAL-smoothness with the default settings. The planning measured by the TPS (TPS-planning) is a value between zero and one representing the ratio between the elapsed time from the start of the movement to the PS and the total

elapsed time for the entire movement. It is an indication of the movement strategy adopted. Values of TPS-planning falling within the range [0.33, 0.5] indicate preplanned movements [32]. Values falling below this interval indicate more time spent in deceleration typical of a guided strategy, whereas values above this interval indicate a ballistic strategy with a shorter deceleration phase. Iwamuro et al. [41] reported that the TPS-planning was able to capture planning changes under different movement directions and dynamics. The association of the chosen metrics with the efficiency, speed, smoothness, and movement planning constructs is such that: 1) the greater the PLR-efficiency, the lower the movement efficiency; 2) the greater the PS-speed, the higher the speed and force generation ability; 3) the greater the SAL-smoothness, the higher the movement smoothness; and 4) TPS-planning values in the [0.33, 0.5] range indicate preplanned movements, TPS-planning < 0.33 indicate a guided strategy, and TPS-planning> 0.5 indicate a ballistic strategy.

E. Hypotheses

In this work, we have four hypotheses. First, the values of the kinematic metrics derived from mocap and Harmony data are expected to be equivalent when simultaneously captured (in-robot condition) in both fast (H1) and slow (H2) speeds. Furthermore, the metrics assessed in Harmony (in-robot condition) are expected to be equivalent to the ones assessed in free motion in both slow (H3) and fast speed, except for PS-speed, where we hypothesize that PS-speed measured in Harmony will be lower than the free-motion value (H4). The reasoning for hypothesis H4 is associated with Harmony's residual friction and noncompensated inertia. Although the residual dynamics is assumed to be negligible for movements at the slow speed, they are likely to alter the human's movement speed in the fast speed condition, where the effect of these components may become significant enough to be perceived as additional load by the human, slowing down movement speed.

F. Statistical Analysis

To test hypotheses H1, H2, H3, and H4 (for PLR-efficiency, SAL-smoothness, and TPS-planning), we adopted an equivalence test using two one-sided tests (TOST) [42], [43]. This test allows us to investigate equivalence between two groups using two one-sided hypothesis tests to verify whether the groups' difference falls within a specified interval. This interval represents a practically important difference also referred as an equivalence interval. We adopted the minimal detectable change (MDC) as the equivalence interval calculated for each metric, target, speed, and condition from the data points obtained with mocap data of all subjects and repetitions pooled together. For hypotheses H3 and H4, we chose the MDC values obtained in free motion as the equivalence interval, which represents the human natural movements. Outliers (i.e., a data point more than 1.5 interquartiles above the upper quartile or below the lower quartile) were excluded from the data pool before the calculation of the MDC but outliers were not excluded for the statistical analysis. The MDC is given by $1.96 \times \text{SEM} \times \sqrt{2}$ [44], where SEM is the standard error of measurement given by the root

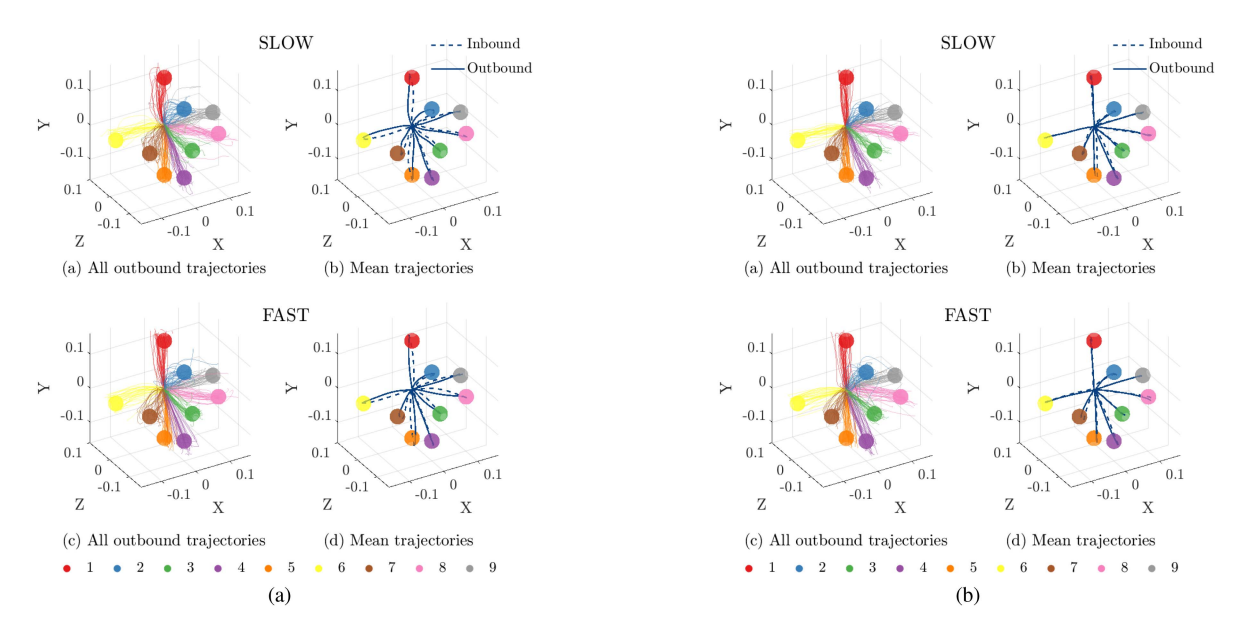


Fig. 4. Outbound hand trajectories measured by mocap of all subjects on the left and the correspondent average trajectories (outbound and inbound) on the right for each speed in the (a) in-robot and (b) free-motion conditions. Each color is associated with one of the nine targets. (a) and (c) All outbound trajectories. (b) and (d) Mean trajectories.

mean of the within-subjects variances. To perform the TOST, we adopted repeated-measures t-tests and $\alpha = 0.05$ to obtain a 90% confidence interval of the difference. Due to the small sample size, we also performed Wilcoxon Signed-Rank tests, which are more conservative and do not require as many assumptions about the samples distribution. In this work, we report the t-test p-values but we only considered a result to be statistically significant when both, the t-test and the Wilcoxon Signed-Rank test give p-values $< \alpha$. To test hypothesis H4 for PS-speed, we adopted repeated-measures t-tests and $\alpha=0.05$. The effect size for this test was calculated with Cohen's d, where we considered d(0.01) = very small, d(0.2) = small, d(0.5) = medium,d(0.8) = large, d(1.2) = very large, and d(2.0) = huge [45].Considering that movement ability might exhibit directional dependence [33], we performed a target-specific analysis. Since a participant's dataset includes four instances of each experimental case (target, speed, and condition), samples were obtained by averaging the values across all repeated instances.

To evaluate consistency between the metrics simultaneously assessed by the two sensing modalities (in-robot condition), we used Bland–Altman plots [46]. These plots indicate average error along with limits of agreement (LOA). The LOA indicate the 95% confidence interval within which discrepancies between the two measurement modalities fall. To generate Bland–Altman plots for each metric individually, we pooled together data points from all targets and all participants grouped by sensing modality (mocap or robot), considering that metric values in repeated targets are averaged for each participant.

The root-mean-squared error (RMSE) and the robot's manipulability will be adopted as supportive metrics in the analysis. The manipulability is calculated from the robot's Jacobian, and the higher its value, the easier it is to impart forces into velocities. The kinematic configuration of a robotic exoskeleton changes its manipulability and influences how well a human can control their arm in different areas of the workspace [47].

III. RESULTS

A qualitative representation of the outbound hand trajectories measured by mocap of all subjects and the correspondent average trajectories are depicted in Fig. 4. The starting point of all trajectories was offset to zero, and the targets represented in the figure serve only as a reference since actual target locations were adjusted for each subject.

The data points for each metric, target, speed, and condition of all subjects and all four repetitions pooled together are represented in Fig. 5 by boxplots grouped by sensing modality. Across all experimental cases, values for PLR (PLR-efficiency), SAL (SAL-smoothness), TPS (TPS-planning), and PS (PS-speed) fell within the ranges [1.02, 1.63], [-2.02, -1.41], [0.15, 0.8], and [0.13, 0.63] in respective order. The overall average values were 1.12, -1.62, 0.47, and 0.27, respectively. Meaningful references and ranges for each metric when existent are indicated in Fig. 5.

The data points excluded from the calculation of the MDC are shown in diamond-shaped markers. The MDC values obtained with data shown in Fig. 5 and adopted in the TOST are depicted in Fig. 6 with green lines and can be inferred from Table II, such that MDC = 2|EI|. Across all experimental cases, the MDC fell within the ranges [0.05, 0.26], [0.16, 0.52], [0.20, 0.55], and [0.04, 0.34] for PLR-efficiency, SAL-smoothness, TPS-planning, and PS-speed, respectively, with averages 0.14, 0.26, 0.34, and 0.12.

The p-values, confidence intervals, equivalence intervals (for equivalence tests), and Cohen's d effect size (for t-tests) are shown in Table II. For equivalence tests, $p = \max(p_1, p_2)$, where p_1 and p_2 correspond to p-values associated with the null hypotheses H_{0_1} and H_{0_2} of the TOST. Instances where the null hypothesis could be rejected ($p \leq 0.05$) are shown in Table II with bolded text and an asterisk next to the p-value. The effect size of all the t-tests with statistical significance (PS-speed, hypothesis H4) was huge, very large, or large. A comparison

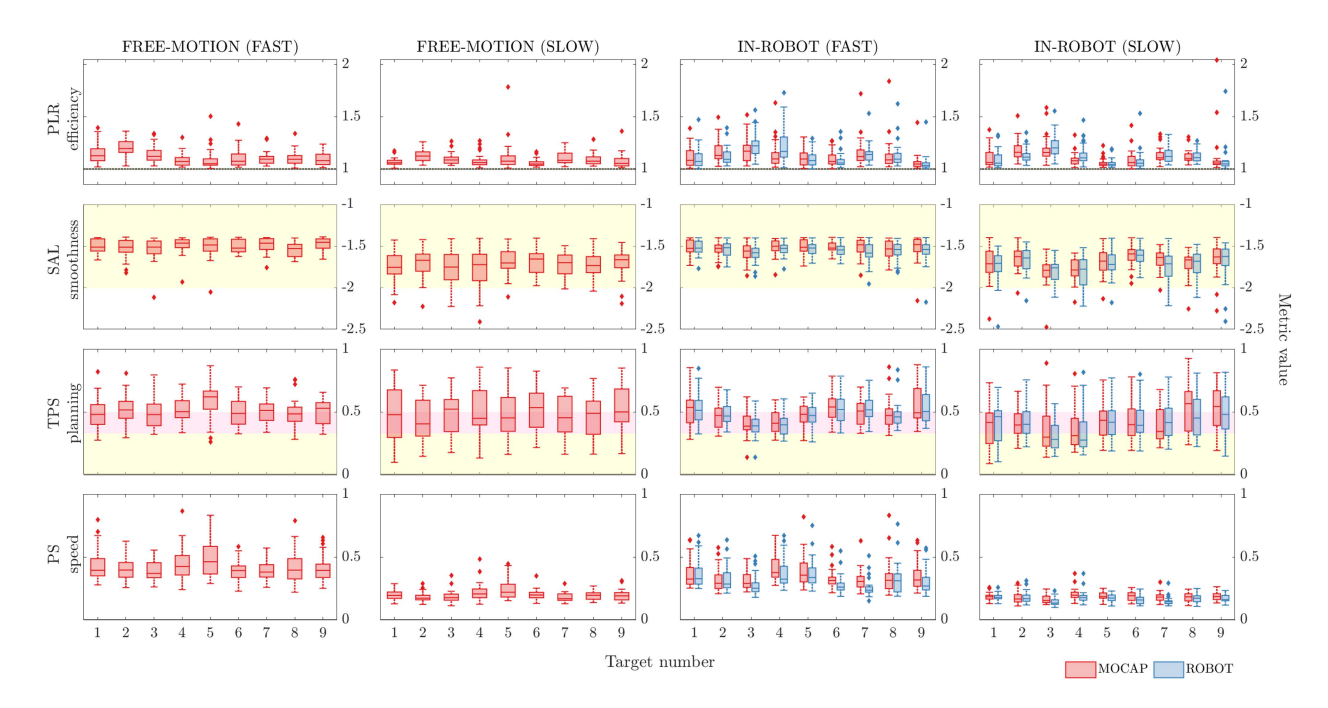


Fig. 5. Distribution of data points for each metric, target, speed, and condition of all subjects and repetitions pooled together. Outliers are shown in diamond-shaped markers. The dotted dark line indicates the minimal value for PLR-efficiency. The yellow, pink, and white areas for TPS-planning indicate guided, preplanned, and ballistic strategy ranges, respectively. For SAL-smoothness, the yellow shaded area indicates the typical range for able-bodied individuals.

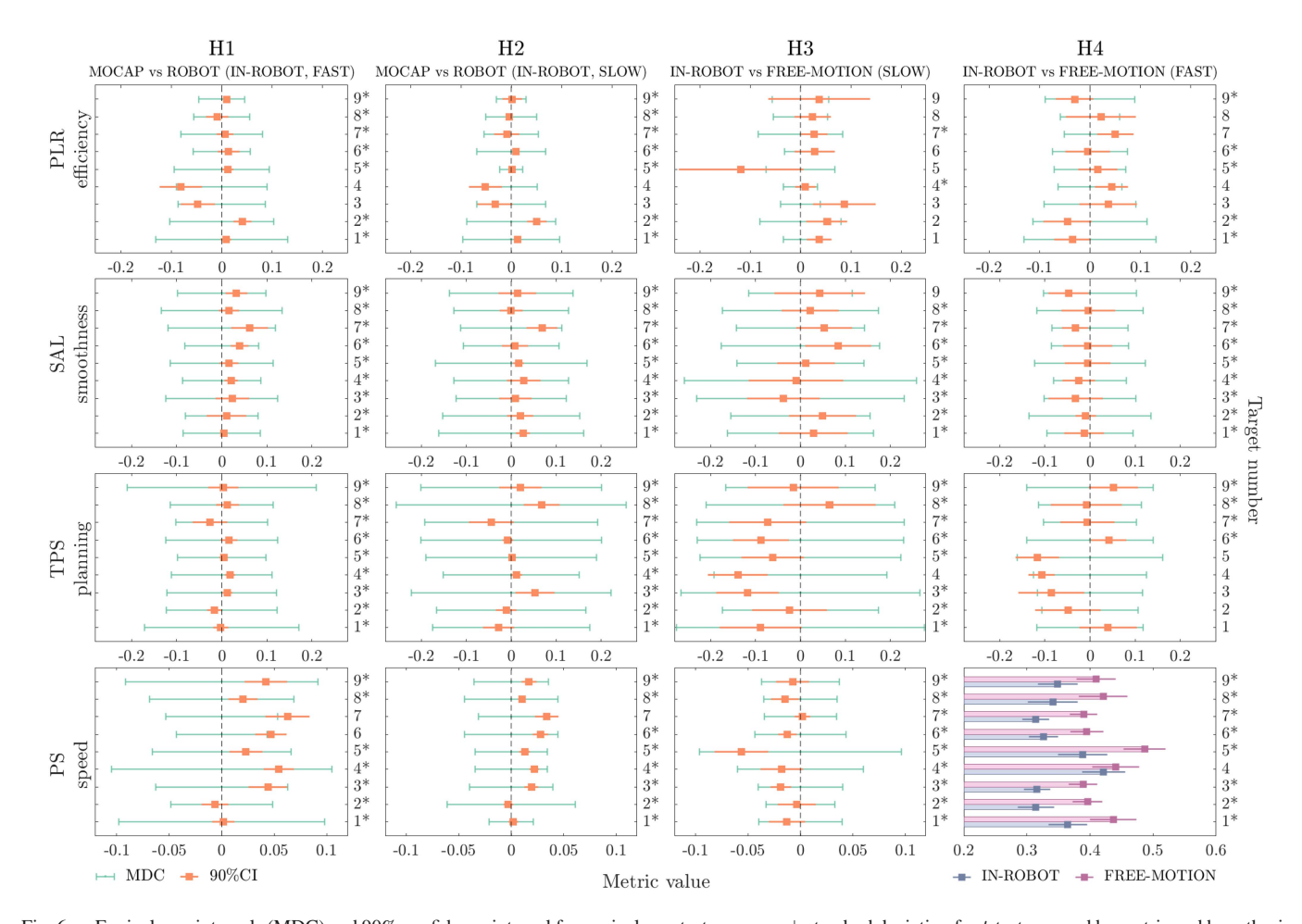


Fig. 6. Equivalence intervals (MDC) and 90% confidence interval for equivalence tests or mean \pm standard deviation for t-test grouped by metric and hypothesis for all targets. Instances with statistical significance in the corresponding hypothesis tests are indicated with an asterisk next to the target number.

Metric	Target	H1		H2			НЗ			H4			
Ž	Ta	EI	p	90% CI	EI	p	90% CI	EI	p	90% CI	EI	p	90% CI
PLR-efficiency	1	±0.131	<.001*	[-0.002,0.019]	±0.096	<.001*	[0.005,0.020]	±0.034	0.604	[0.013,0.062]	±0.130	<.001*	[-0.071,0.001]
	2	± 0.103	<.001*	[0.023, 0.058]	±0.089	<.001*	[0.032, 0.070]	± 0.080	0.119	[0.012, 0.093]	± 0.113	0.015*	[-0.092,0.004]
	3	±0.087	0.033	[-0.081,-0.014]	±0.069	0.044	[-0.067,0.003]	± 0.039	0.907	[0.025, 0.149]	±0.091	0.056	[-0.021,0.094]
	4	±0.090	0.356	[-0.123,-0.039]	±0.052	0.490	[-0.084,-0.018]	± 0.033	0.034*	[-0.011, 0.031]	±0.063	0.137	[0.010,0.076]
	5	± 0.094	<.001*	[0.000, 0.023]	± 0.023	<.001*	[-0.003,0.008]	± 0.068	0.765	[-0.242,0.006]	± 0.071	0.016*	[-0.023,0.055]
	6	± 0.056	<.001*	[-0.008,0.035]	± 0.068	<.001*	[0.003, 0.015]	± 0.032	0.440	[-0.012,0.068]	± 0.074	0.010*	[-0.048,0.039]
	7	± 0.081	<.001*	[-0.010, 0.023]	± 0.054	0.006*	[-0.034,0.017]	± 0.084	<.001*	[-0.000, 0.054]	±0.051	0.482	[0.014,0.086]
	8	± 0.056	0.002*	[-0.031,0.013]	± 0.050	<.001*	[-0.010, 0.003]	± 0.054	0.080	[-0.011,0.060]	±0.059	0.174	[-0.048,0.091]
	9	± 0.046	<.001*	[0.006, 0.013]	±0.029	0.017*	[-0.017, 0.021]	± 0.056	0.367	[-0.064,0.138]	± 0.088	0.010*	[-0.067,0.006]
	1	± 0.086	<.001*	[0.000,0.010]	± 0.162	<.001*	[0.011,0.042]	± 0.162	0.007*	[-0.048,0.106]	± 0.095	0.005*	[-0.057,0.031]
	2	± 0.081	0.010*	[-0.033,0.055]	± 0.153	<.001*	[-0.009,0.049]	± 0.155	<.001*	[-0.025, 0.124]	± 0.135	<.001*	[-0.032,0.013]
SAL-smoothness	3	± 0.124	<.001*	[-0.014,0.061]	± 0.122	<.001*	[-0.026, 0.046]	± 0.231	0.001*	[-0.118,0.043]	± 0.102	0.033*	[-0.092, 0.028]
츀	4	± 0.087	<.001*	[0.006, 0.036]	± 0.128	<.001*	[-0.009, 0.066]	± 0.258	0.001*	[-0.115,0.096]	± 0.081	0.010*	[-0.060, 0.012]
ĕ	5	± 0.114	<.001*	[-0.005,0.037]	± 0.168	<.001*	[0.004, 0.029]	± 0.141	0.003*	[-0.052, 0.077]	± 0.123	0.002*	[-0.056,0.045]
IS.	6	± 0.082	<.001*	[0.020, 0.060]	± 0.106	<.001*	[-0.021, 0.038]	± 0.176	<.001*	[0.010, 0.158]	± 0.085	0.013*	[-0.059, 0.050]
Ϋ́	7	± 0.120	<.001*	[0.021, 0.103]	± 0.113	<.001*	[0.035, 0.103]	± 0.143	<.001*	[-0.010, 0.116]	± 0.085	0.006*	[-0.062,-0.003]
0,	8	± 0.135	<.001*	[-0.007,0.039]	± 0.128	<.001*	[-0.026, 0.025]	± 0.173	<.001*	[-0.042,0.085]	± 0.118	0.004*	[-0.064,0.056]
	9	±0.099	<.001*	[0.009, 0.057]	± 0.137	<.001*	[-0.027, 0.055]	± 0.115	0.110	[-0.057,0.144]	± 0.103	0.026*	[-0.092,-0.003]
	1	± 0.171	<.001*	[-0.019,0.015]	± 0.175	<.001*	[-0.063,0.007]	±0.276	0.003*	[-0.180,0.003]	±0.117	0.027	[-0.024,0.104]
	2	± 0.123	<.001*	[-0.033, 0.000]	± 0.167	<.001*	[-0.034, 0.012]	± 0.174	0.006*	[-0.107, 0.059]	± 0.107	0.088	[-0.122,0.024]
50	3	± 0.122	<.001*	[0.002, 0.024]	± 0.222	<.001*	[0.010, 0.097]	± 0.266	0.003*	[-0.187,-0.048]	± 0.116	0.228	[-0.159,-0.012]
. <u>ii</u>	4	± 0.112	<.001*	[0.008, 0.030]	± 0.151	<.001*	[0.001, 0.024]	± 0.192	0.086	[-0.205,-0.073]	± 0.125	0.143	[-0.137,-0.078]
pla	5	± 0.098	<.001*	[-0.005, 0.014]	± 0.190	<.001*	[-0.006, 0.011]	± 0.224	0.002*	[-0.132,0.008]	± 0.162	0.060	[-0.165,-0.069]
TPS-planning	6	± 0.124	<.001*	[-0.002,0.035]	± 0.201	<.001*	[-0.019, 0.004]	± 0.230	0.002*	[-0.150, -0.025]	± 0.140	<.001*	[0.003, 0.081]
E	7	± 0.102	0.004*	[-0.065, 0.012]	± 0.192	<.001*	[-0.094,0.005]	± 0.231	0.005*	[-0.159,0.013]	± 0.103	0.009*	[-0.066,0.054]
	8	± 0.114	<.001*	[-0.012,0.038]	± 0.255	<.001*	[0.028, 0.107]	± 0.210	<.001*	[-0.038, 0.167]	± 0.115	0.019*	[-0.087, 0.071]
	9	±0.209	<.001*	[-0.029,0.038]	± 0.200	<.001*	[-0.027,0.068]	± 0.167	0.013*	[-0.117,0.086]	± 0.140	<.001*	[-0.002,0.106]
		EI	p	90% CI	EI	p	90% CI	EI	p	$90\% \ CI$	d	p	95% CI
	1	±0.098	<.001*	[-0.009,0.012]	± 0.021	<.001*	[-0.002,0.007]	± 0.040	0.011*	[-0.030,0.004]	1.416	0.003*	$[-\infty, -0.038]$
	2	± 0.048	<.001*	[-0.019,0.006]	± 0.061	<.001*	[-0.007, 0.002]	± 0.033	0.009*	[-0.022, 0.015]	2.280	<.001*	$[-\infty, -0.058]$
	3	± 0.063	<.001*	[0.026, 0.062]	± 0.040	<.001*	[0.013, 0.026]	± 0.040	0.002*	[-0.029, -0.009]	2.066	<.001*	$[-\infty, -0.049]$
seq	4	± 0.105	<.001*	[0.040, 0.069]	± 0.035	<.001*	[0.018, 0.026]	± 0.060	0.003*	[-0.038, 0.002]	0.484	0.107	$[-\infty, 0.007]$
PS-speed	5	± 0.066	<.001*	[0.007, 0.039]	± 0.035	<.001*	[0.008, 0.018]	± 0.097	0.010*	[-0.082,-0.031]	0.909	0.019*	$[-\infty, -0.026]$
	6	± 0.043	0.682	[0.032,0.062]	± 0.044	<.001*	[0.020, 0.036]	± 0.043	<.001*	[-0.021, -0.003]	1.114	0.008*	$[-\infty, -0.027]$
	7	±0.053	0.788	[0.042,0.084]	± 0.031	0.650	[0.022, 0.045]	± 0.034	<.001*	[-0.006, 0.009]	2.488	<.001*	$[-\infty, -0.056]$
	8	±0.069	<.001*	[0.006, 0.034]	± 0.045	<.001*	[0.007, 0.014]	± 0.035	0.011*	[-0.028, -0.002]	3.587	<.001*	$[-\infty, -0.065]$
	9	± 0.091	<.001*	[0.022, 0.062]	± 0.035	<.001*	[0.010, 0.024]	± 0.037	0.004*	[-0.023,0.008]	1.331	0.004*	$[-\infty, -0.030]$

TABLE II DESCRIPTIVE STATISTICS FOR PLR-EFFICIENCY, SAL-SMOOTHNESS, TPS-PLANNING, AND PS-SPEED

EI - Equivalence Interval, CI - Confidence interval, p - max p-value (TOST) or p-value (t-test), d - Cohen's d Hypotheses summary (alternative hypothesis H_a) - H1: $-MDC/2 \le (\mu_{IfM} - \mu_{IfR}) \le MDC/2$, H2: $-MDC/2 \le (\mu_{IsM} - \mu_{IsR}) \le MDC/2$, H3: $-MDC/2 \le (\mu_{IsM} - \mu_{IsR}) \le MDC/2$, and H4 (all but PS-speed): $-MDC/2 \le (\mu_{IfM} - \mu_{FfM}) \le MDC/2$ or H4 (PS-speed): $(\mu_{IfM} - \mu_{FfM}) \le 0$,

with I (in-robot), F (free-motion), f (fast-speed), s (slow-speed), M (mocap), R (robot).

between the 90% confidence intervals and MDC (for equivalent tests) or mean and standard deviation of each condition (for t-tests) are illustrated in Fig. 6.

From Fig. 6 and Table II, we can infer that the differences between the sensing modalities are smaller than the practically important difference when simultaneously captured (i.e., in the in-robot condition) in all targets for TPS-planning and SALsmoothness. The same applies for PLR-efficiency excluding targets 3 and 4, and for PS-speed excluding targets 6 and 7 for fast speed and target 7 for slow speed. As for the hypothesis H3, we can infer that differences between values captured in the in-robot and free-motion conditions are smaller than the practically important difference in most targets in all metrics, except PLR-efficiency. We cannot infer that differences between the two conditions are smaller than the practically important difference in target 9 for SAL-smoothness and in target 4 in TPS-planning. For PLR-efficiency, we can infer that the differences between the two conditions are smaller than the practically important difference only in targets 4 and 7. Regarding hypothesis H4, we can infer that the differences between the two conditions are smaller than the practically important difference in all targets for SAL-smoothness, in targets 1, 2, 5, 6, and 9 for PLR-efficiency, and in targets 6 through 9 for TPS-planning. Furthermore, we can infer that PS-speed obtained in the free-motion condition is larger than in the in-robot for all targets except 4.

The Bland–Altman plots indicating the LOA are shown in Fig. 7. The data points are indicated with circle- or diamondshaped markers for fast and slow speeds, respectively, and are shown in target-specific colors. From these plots, the discrepancies between the two measurement modalities (mocap and robot) for PLR-efficiency, PS-speed, TPS-planning, and SALsmoothness fall within the ranges [-0.09, 0.08], [-0.03, 0.07],[-0.09, 0.10], and [-0.06, 0.11], respectively.

The RMSE between mocap and the robot's hand-velocity profiles are represented in Fig. 8 for each target. The highest RMSE is observed in target 7, followed by targets 3, 4, and 6. Finally, the average manipulability from the initial position toward each target is illustrated in Fig. 9. These values represent the length of the manipulability ellipsoid in each direction. The targets directions with the highest manipulabilities were 1, 5, 6, and 9.

IV. DISCUSSION

In this work, we presented a quantitative comparison of kinematic metrics measured by Harmony and an optical mocap system during reaching movements. We previously presented a similar quantitative comparison focused on joint angles [30]. Here, we extended the analysis to four Cartesian-space metrics that are directly associated with movement quality. In addition,

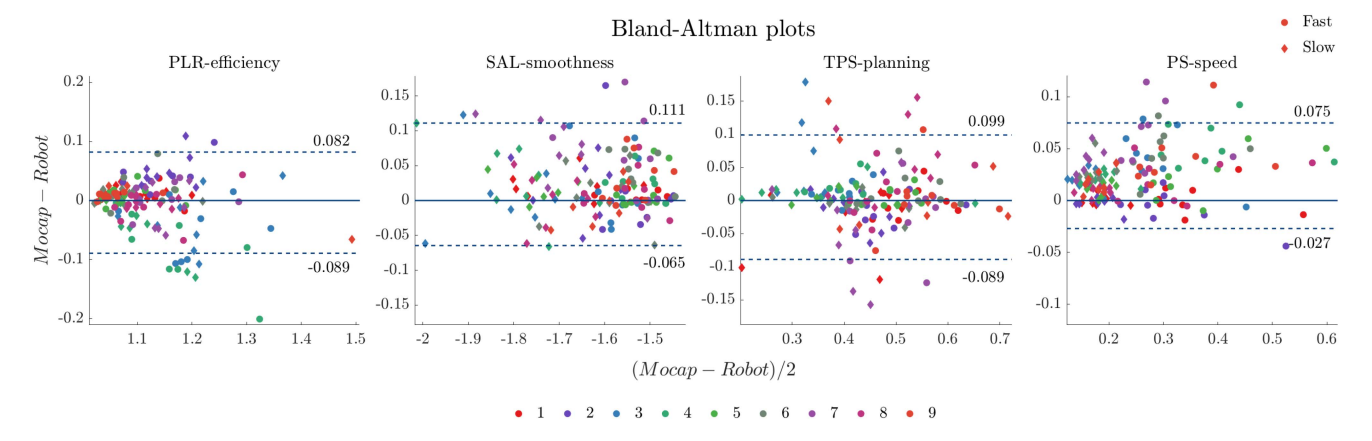


Fig. 7. Bland–Altman plots from data captured during the in-robot conditions. Each color is associated with one of the nine targets. Dotted lines represent LOA with corresponding values indicated directly above or below the line.

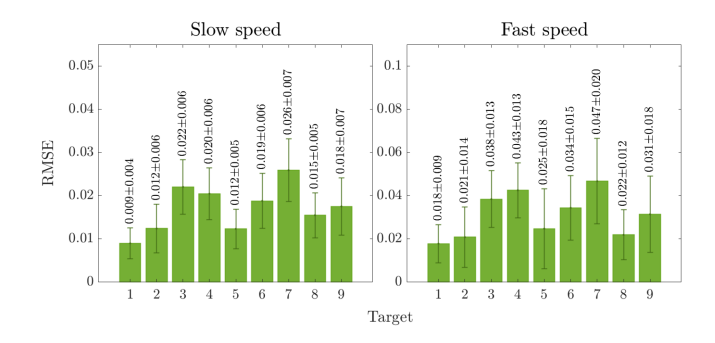


Fig. 8. RMSE of the hand-velocity profiles simultaneously captured by Harmony and mocap per target and speed.

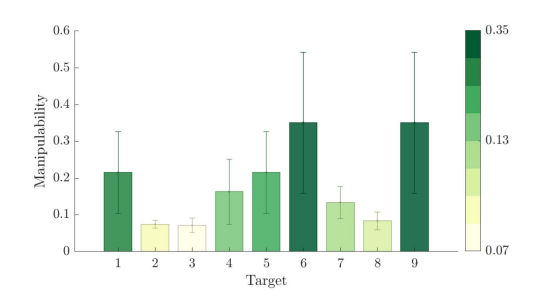


Fig. 9. Average manipulability of Harmony toward each of the nine targets.

we performed a novel analysis to investigate Harmony's ability to accurately capture the human movement in free motion.

A. Qualitative Observations

Based on a visual inspection of Fig. 4, Cartesian-space trajectories executed in Harmony in both the fast and slow speeds exhibited larger spatial distribution than in free motion. This variability might be associated with changes in movement execution caused by adaptation to a new dynamic environment. Although the hand trajectories in the robot appear to exhibit higher variability than those out of the robot, this difference was not reflected in the metrics of movement quality (see Fig. 5). This indicates that although hand trajectory might change in the robot, that does not necessarily affect certain aspects of the underlying motor behavior.

From the boxplots in Fig. 5, the PLR (PLR-efficiency) exhibited higher medians and larger variability in the fast speed than at the slow speed, but overall values are all close to the minimal value of 1. The higher medians could be associated with movement corrections due to overshoots, often present in fast speeds [48]. These overshooting trajectories cause larger variability across participants since each might choose different movement corrections. The PS (PS-speed) also exhibited larger variability at the fast speed compared to the slow speed, which was expected since the participants were asked to move as fast as possible during the fast speed condition. Furthermore, the PS-speed medians demonstrate that the speeds executed were consistent with the desired speeds.

In contrast to these observations, the TPS (TPS-planning) and SAL (SAL-smoothness) exhibit higher variability at the slow speed rather than at the fast speed. The higher variability in TPS-planning indicates that participants might have changed movement strategies more often during slow movements. In addition, the medians for SAL-smoothness are lower in the slow speed indicating lower smoothness. These results suggest that more submovements are present at slow speeds, which is consistent with observations in a different study [48]. The data points for SAL-smoothness confirmed that the range [-2, -1] is typical for able-bodied individuals [21]. The results for TPS-planning suggest that humans tend to choose a ballistic strategy for fast movements and a preplanned strategy for slow movements.

B. Hypotheses H1 and H2

Results in the first two columns of Table II and Fig. 6 demonstrate that in most cases, both the sensing modalities give equivalent observations when simultaneously captured in Harmony (i.e., in the in-robot condition). These results indicate that Harmony is in most part sufficiently accurate to measure kinematic parameters associated with movement quality. In the in-robot condition, some instances such as PLR-efficiency targets 3 and 4, and PS-speed targets 6 and 7, did not present evidence for equivalence between robot and mocap. We speculate that this

is associated with discrepancies in the kinematic model used to obtain the hand-position from Harmony's joint angles. We used a tape measure to determine each participant's body dimensions adopted in the kinematic model shown in Table I, and this method is susceptible to human error. Inaccuracies in the kinematic model could cause the hand-trajectory in Cartesian space to be slightly different between robot and mocap. This can be observed in Fig. 8, where the highest RMSE is observed in target 7, followed by targets 3, 4, and 6. These are the same targets aforementioned, where we did not find evidence of equivalence for PLR-efficiency and PS-speed. The PLR-efficiency and PS-speed are directly associated with Cartesian space positions, whereas TPS-planning and SAL-smoothness are associated with time and frequency features of the movement and less likely to be affected by position discrepancies. Therefore, the results from the equivalence tests are coherent with the deviations observed in Fig. 8. A more accurate measurement of the human body dimensions is a potentially trivial solution to minimize discrepancies in the position-dependent metrics, but measurement errors cannot be completely mitigated. Thus, target directions with low kinematic discrepancies should be prioritized to obtain a more accurate measure of the position-dependent metrics. From our results, target 1 presented the lowest difference followed by 2, 5, 8, and 9.

The LOA shown in the Bland-Altman plots in Fig. 7 all fall within the ranges, or are lower than the minimal value, of each respective MDC. This is a supporting result showing that Harmony is comparable with mocap to measure kinematic parameters associated with movement quality. The LOA for PS-speed are centered around a positive value, which suggests that PS-speed obtained from mocap are larger than the ones obtained from Harmony, which is consistent with Fig. 8.

C. Hypotheses H3 and H4

Results in the third column of Table II and Fig. 6 demonstrate that observations captured in and out of the robot in the slow speed are equivalent in most targets for SAL-smoothness, TPS-planning, and PS-speed. The same was not observed for PLR-efficiency, except in rare occasions (targets 4 and 7). Results in the last column of Table II and Fig. 6 demonstrate similar patterns for SAL-smoothness and PLR-efficiency, i.e., observations captured in and out of the robot in the fast speed are equivalent in most targets for SAL-smoothness but not for PLR-efficiency, except in a few occasions (targets 1, 2, 5, 6, and 9). These results suggest that in the most part, Harmony can accurately capture the natural (i.e., free motion) movement speed, planning, and smoothness of a human during the slow speed, and the natural movement smoothness also during the fast speed. Furthermore, movement efficiency (PLR-efficiency) captured in Harmony may be lower than a human's natural movement efficiency, regardless of the speed. TPS-planning values demonstrated that movement planning captured in Harmony during the fast speed is only consistent with free motion for movements in the horizontal but not in the vertical plane. Finally, PS-speed values indicate that the speed captured in Harmony during the fast speed is significantly lower than the free-motion movement speed, which endorses our initial hypothesis that Harmony's residual friction and noncompensated inertia significantly alter the human's natural movement speed.

We suspect that the unexpected discrepancies found for PLRefficiency and TPS-planning are associated with two factors: 1) the robot's residual gravity pull; and 2) manipulability. The residual gravity pull stems from errors in the dynamics model, which could lead to either over or undercompensating for the robot's weight. It is likely that the weight was undercompensated and the residual gravity pull was perceived by the human as an extra load pulling down. The results for PLR-efficiency at the slow speed show that participants were surprisingly more efficient in Harmony than in free motion for target 5 (see Fig. 6), which was located right below the initial position. Furthermore, the PS-speed shows that movements in Harmony were slightly faster toward target 5 compared to free motion. In contrast, PLRefficiency values in the opposite direction, i.e., target 1, show that participants were less efficient in Harmony than in free motion. This is consistent with our speculation since the extra weight would assist toward target 5 and resist toward target 1. Moreover, the additional load would represent an external perturbation, but in fast movements, the additional inertia may dampen the effects of these perturbations in motor coordination. In contrast, the perturbation from the additional load could affect the human's motor coordination at the slow speed, which could explain why the movement efficiency measured in Harmony during the slow speed is lower than in free motion. In addition to that, our results for TPS-planning endorse the presence of an extra load when in the robot since the values measured in Harmony were equivalent to the free-motion values for the slow speed but not for the fast speed on targets in the vertical direction (i.e., 1, 2, 4, 5). This indicates that movement planning in the vertical direction captured in Harmony was the same as free-motion planning at a slow speed, but participants spent more time in deceleration than in acceleration during the fast speed.

The other factor we speculate being related to discrepancies in PLR-efficiency is the robot's manipulability. The targets directions with the highest levels of manipulability were 1, 5, 6, and 9 (see Fig. 9), indicating that it is easier to impart forces into velocities toward these targets directions. Results in Fig. 6 for PLR-efficiency in fast speed show that the movement efficiency in Harmony was equivalent to free-motion in all of these targets, but not to most of the remaining ones. The values found indicate that for targets 3, 4, 7, and 8, the movement efficiency measured in Harmony are lower than free-motion. Both of these findings support the idea that manipulability interferes with movement efficiency at the fast speed. The slow speed requires less forces from the human, and the interference from manipulability in this case would be less significant.

D. Recommendations

In light of the findings of this study, we recommend assessment of position-dependent metrics such as PLR-efficiency and PS-speed to be performed in a plane parallel to the coronal, preferably in the vertical direction. We suggest that information of manipulability should be adopted to guide assessment

of movement efficiency. Directions with higher manipulability should be preferred since they are less likely to reduce efficiency compared to free-motion. In addition to that, we recommend velocities comparable with the ones in activities of daily living (ADL) [35], [36] for the assessment of movement efficiency since that minimizes the influence of residual gravity pull in the human's movements. In contrast, we suggest much lower velocities (a half or a third of the ADL speeds) to assess movement speed since that minimizes the effects of residual friction and inertia in the robot. Furthermore, we recommend metrics of movement planning such as TPS-planning to be measured in the horizontal plane, where residual gravity pull is less likely to influence the results. Finally, movement smoothness measured by SAL-smoothness has demonstrated robustness across all directions and movement speeds and can be adopted in a variety of reaching tasks for the assessment.

E. Limitations

The results of this study suggest that Harmony is a robust tool for the assessment of movement smoothness, but it has limitations when measuring efficiency, speed, and planning. When assessing these metrics, the robot might provide measurements different than the ones obtained with mocap or it might influence the human's natural movement behavior in specific conditions. However, as demonstrated in previous works [30], mocap systems also present limitations and may not give exact measurements of the human motion. Furthermore, although Harmony may affect human's natural movement behavior in certain conditions, using Harmony as a tool is beneficial because of its simultaneous capability to provide training and continuous assessment. In summary, to determine whether Harmony is an appropriate tool for the assessment in a specific investigation, it is important to evaluate if the priority is to provide a highly accurate measurement of the human's movement behavior or to provide continuous and efficient measurements without additional time.

This work has a limitation related to the specificity of the assessment task adopted, which reduces choices of kinematic metrics to ones associated with point-to-point reaching. However, this is a reasonable choice given that reaching is a fundamental component of various activities of daily living and is extensively adopted in studies of upper-extremity movement for the assessment of a variety of kinematic metrics [13], [49].

V. CONCLUSION

In this study, we compared kinematic metrics obtained using the Harmony exoskeleton with an optical mocap system measured during a point-to-point task. We carried out an experiment and analyzed the data collected from eight able-bodied participants in and out of the robot and at fast and slow speeds. The fast speed was comparable with ADLs and the slow speed was about four times slower than the fast. Results suggest that Harmony was sufficiently accurate to measure kinematic parameters associated with movement quality since values assessed by the robot were consistent with mocap. Harmony could accurately capture the human's natural movement smoothness regardless of the speed and direction. The robot also captured the human's natural movement speed and planning during the slow

speed. Although these conclusions are based upon data acquired from able-bodied individuals, they may be generalized to stroke patients because the consistency between the robot and mocap is independent of the human's ability and the limitations associated with movement impairments may be handled independently from the robot. This work provided useful insights and guidance for the use of Harmony for kinematic assessment. Our long-term goal is to provide clinically relevant and accurate assessments while delivering several rehabilitation training approaches. Such an ability may help with the identification of key ingredients for maximizing the effectiveness of robot-mediated training for upper-body stroke recovery.

REFERENCES

- D. Mozaffarian et al., "Executive summary: Heart disease and stroke statistics-2016 update: A report from the American Heart Association," *Circulation*, vol. 133, no. 4, pp. 447–454, 2016.
- [2] A. M. Hadjiosif, M. Branscheidt, M. A. Anaya, K. D. Runnalls, J. Keller, and A. J. Bastian, "Dissociation between abnormal motor synergies and impaired reaching dexterity after stroke," *J. Neuriophysiol.*, vol. 127, no. 4, pp. 856–868, 2022.
- [3] K. Sawner, J. M. LaVigne, and S. Brunnstrom, Movement Therapy in Hemiplegia: A Neurophysiological Approach. Philadelphia, PA, USA: Lippincott, 1992.
- [4] C. Lang, R. Birkenmeier, and A. O. T. Association, Upper-Extremity Task-Specific Training After Stroke or Disability: A Manual for Occupational Therapy and Physical Therapy. Bethesda, MD, USA: OTA Press, 2014.
- [5] P. Raghavan, "Upper limb motor impairment post stroke," Phys. Med. Rehabil. Clin. North Amer., vol. 26, no. 4, pp. 599–610, 2016.
- [6] J.-M. Gracies, "Pathophysiology of impairment in patients with spasticity and use of stretch as a treatment of spastic hypertonia," *Phys. Med. Rehabil. Clin. North Amer.*, vol. 12, no. 4, pp. 747–768, Nov. 2001.
- [7] C. E. Lang, J. M. Wagner, D. F. Edwards, and A. W. Dromerick, "Upper extremity use in people with hemiparesis in the first few weeks after stroke," J. Neurol. Phys. Ther., vol. 31, no. 2, pp. 56–63, 2007.
- [8] D. U. Jette, J. Halbert, C. Iverson, E. Miceli, and P. Shah, "Use of standardized outcome measures in physical therapist practice: Perceptions and applications," *Phys. Ther.*, vol. 89, no. 2, pp. 125–135, 2009.
- [9] C. E. Lang, M. D. Bland, R. R. Bailey, S. Y. Schaefer, and R. L. Birkenmeier, "Assessment of upper extremity impairment, function, and activity after stroke: Foundations for clinical decision making," *J. Hand Ther.*, vol. 26, no. 2, pp. 104–115, Apr. 2013.
- [10] N. Yozbatiran, L. Der-Yeghiaian, and S. C. Cramer, "A standardized approach to performing the action research arm test," *Neurorehabilitation Neural Repair*, vol. 22, no. 1, pp. 78–90, 2008.
- [11] J. M. Linacre, A. W. Heinemann, B. D. Wright, C. V. Granger, and B. B. Hamilton, "The structure and stability of the functional independence measure," *Arch. Phys. Med. Rehabil.*, vol. 75, no. 2, pp. 127–132, Feb. 1994.
- [12] D. J. Gladstone, C. J. Danells, and S. E. Black, "The Fugl-Meyer assessment of motor recovery after stroke: A critical review of its measurement properties," *Neurorehabilitation Neural Repair*, vol. 16, no. 3, pp. 232–240, 2002.
- [13] N. Nordin, S. Q. Xie, B. Wünsche, and B. Wunsche, "Assessment of movement quality in robot- assisted upper limb rehabilitation after stroke: A review," J. Neuroeng. Rehabil., vol. 11, no. 1, 2014, Art. no. 137.
- [14] A. Schwarz, C. M. Kanzler, O. Lambercy, A. R. Luft, and J. M. Veerbeek, "Systematic review on kinematic assessments of upper limb movements after stroke," *Stroke*, vol. 50, no. 3, pp. 718–727, Mar. 2019.
- [15] J. van Kordelaar et al., "Assessing longitudinal change in coordination of the paretic upper limb using on-site 3-dimensional kinematic measurements," *Phys. Ther.*, vol. 92, no. 1, pp. 142–151, Jan. 2012.
- [16] T. Kitago, J. Liang, V. S. Huang, S. Hayes, P. Simon, and L. Tenteromano, "Improvement after constraint-induced movement therapy: Recovery of normal motor control or task-specific compensation?," *Neurorehabilita*tion Neural Repair, vol. 27, no. 2, pp. 99–109, 2013.
- [17] J. Mehrholz, M. Pohl, T. Platz, J. Kugler, and B. Elsner, "Electromechanical and robot-assisted arm training for improving activities of daily living, arm function, and arm muscle strength after stroke," *Cochrane Database Systematic Rev.*, no. 9, 2018, Art. no. CD006876, doi: 10.1002/14651858.CD006876.pub5.

- [18] R. A. Gopura, D. S. Bandara, K. Kiguchi, and G. K. Mann, "Developments in hardware systems of active upper-limb exoskeleton robots: A review," *Robot. Auton. Syst.*, vol. 75, pp. 203–220, Jan. 2016.
- [19] Hocoma, "Armeo Power," 2023. Accessed: Oct. 25, 2021. [Online]. Available: https://www.hocoma.com/us/solutions/armeo-power/
- [20] Kinetec, "ALEx.," 2017. Accessed: Oct. 25, 2021. [Online]. Available: http://www.wearable-robotics.com/kinetek/products/alex/
- [21] C. G. Rose, E. Pezent, C. K. Kann, A. D. Deshpande, and M. K. O'Malley, "Assessing wrist movement with robotic devices," *IEEE Trans. Neural Syst. Rehabil. Eng.*, vol. 26, no. 8, pp. 1585–1595, Aug. 2018.
- [22] D. Campolo, D. Accoto, D. Formica, and E. Guglielmelli, "Intrinsic constraints of neural origin: Assessment and application to rehabilitation robotics," *IEEE Trans. Robot.*, vol. 25, no. 3, pp. 492–501, Jun. 2009.
- [23] N. L. Tagliamonte, M. Scorcia, D. Formica, D. Campolo, and E. Guglielmelli, "Effects of impedance reduction of a robot for wrist rehabilitation on human motor strategies in healthy subjects during pointing tasks," Adv. Robot., vol. 25, no. 5, pp. 537–562, 2011.
- [24] M. A. Gull, S. Bai, and T. Bak, "A review on design of upper limb exoskeletons," *Robotics*, vol. 9, no. 1, pp. 1–35, 2020.
- [25] T. Nef, M. Mihelj, G. Kiefer, C. Perndl, R. Müller, and R. Riener, "ARMin Exoskeleton for arm therapy in stroke patients," in *Proc. IEEE 10th Int. Conf. Rehabil. Robot.*, 2007, pp. 68–74.
- [26] F. Just et al., "Exoskeleton transparency: Feed-forward compensation vs. disturbance observer," *At-Automatisierungstechnik*, vol. 66, no. 12, pp. 1014–1026, 2018.
- [27] J. C. Perry, J. Rosen, and S. Burns, "Upper-limb powered exoskeleton design," *IEEE/ASME Trans. Mechatron.*, vol. 12, no. 4, pp. 408–417, Aug. 2007.
- [28] B. Kim and A. D. Deshpande, "An upper-body rehabilitation exoskeleton Harmony with an anatomical shoulder mechanism: Design, modeling, control, and performance evaluation," *Int. J. Robot. Res.*, vol. 36, no. 4, pp. 414–435, 2017.
- [29] B. Kim and A. D. Deshpande, "Controls for the shoulder mechanism of an upper-body exoskeleton for promoting scapulohumeral rhythm," in *Proc. IEEE Int. Conf. Rehabil. Robot.*, 2015, pp. 538–542.
- [30] A. C. De Oliveira, J. S. Sulzer, and A. D. Deshpande, "Assessment of upper-extremity joint angles using Harmony exoskeleton," *IEEE Trans. Neural Syst. Rehabil. Eng.*, vol. 29, pp. 916–925, 2021, doi: 10.1109/TNSRE.2021.3074101.
- [31] S. Balasubramanian, A. Melendez-Calderon, and E. Burdet, "A robust and sensitive metric for quantifying movement smoothness," *IEEE Trans. Biomed. Eng.*, vol. 59, no. 8, pp. 2126–2136, Aug. 2012.
 [32] C. A. Trombly and C. Y. Wu, "Effect of rehabilitation tasks on organi-
- [32] C. A. Trombly and C. Y. Wu, "Effect of rehabilitation tasks on organization of movement after stroke," *Amer. J. Occup. Ther.*, vol. 53, no. 4, pp. 333–344, 1999.
- [33] A. Panarese, R. Colombo, I. Sterpi, F. Pisano, and S. Micera, "Tracking motor improvement at the subtask level during robot-aided neurorehabilitation of stroke patients," *Neurorehabilitation Neural Repair*, vol. 26, no. 7, pp. 822–833, 2012.
- [34] M. Spong and M. Vidyasagar, Robot Dynamics and Control. Hoboken, NJ, USA: Willey, 1989.

- [35] I. A. Mesquita et al., "Comparison of upper limb kinematics in two activities of daily living with different handling requirements," *Hum. Movement Sci.*, vol. 72, 2020, Art. no. 102632.
- [36] P. Gulde, S. Schmidle, A. Aumüller, and J. Hermsdörfer, "The effects of speed of execution on upper-limb kinematics in activities of daily living with respect to age," *Exp. Brain Res.*, vol. 237, no. 6, pp. 1383–1395, 2019.
- [37] K. Ghonasgi, C. G. Rose, A. C. De Oliveira, R. J. Varghese, and A. D. Deshpande, "Design and validation of a novel exoskeleton hand interface: The eminence grip," in *Proc. IEEE Int. Conf. Robot. Automat.*, 2021, pp. 3707–3713.
- [38] M. C. Cirstea and M. F. Levin, "Compensatory strategies for reaching in stroke," *Brain*, vol. 123, no. 5, pp. 940–953, May 2000.
- [39] J.-J. Chang, W.-L. Tung, W.-L. Wu, M.-H. Huang, and F.-C. Su, "Effects of robot-aided bilateral force-induced isokinetic arm training combined with conventional rehabilitation on arm motor function in patients with chronic stroke," *Arch. Phys. Med. Rehabil.*, vol. 88, no. 10, pp. 1332–1338, Oct. 2007.
- [40] C. Bosecker, L. Dipietro, B. Volpe, and H. I. Krebs, "Kinematic robot-based evaluation scales and clinical counterparts to measure upper limb motor performance in patients with chronic stroke," *Neurorehabilitation Neural Repair*, vol. 24, no. 1, pp. 62–69, 2010.
- [41] B. T. Iwamuro, E. G. Cruz, L. L. Connelly, H. C. Fischer, and D. G. Kamper, "Effect of a gravity-compensating orthosis on reaching after stroke: Evaluation of the therapy assistant WREX," Arch. Phys. Med. Rehabil., vol. 89, no. 11, pp. 2121–2128, Nov. 2008.
- [42] J. L. Rogers, K. I. Howard, and J. T. Vessey, "Using significance tests to evaluate equivalence between two experimental groups.," *Psychol. Bull.*, vol. 113, no. 3, 1993, Art. no. 553.
- [43] E. J. Mascha and D. I. Sessler, "Equivalence and noninferiority testing in regression models and repeated-measures designs," *Anesth. Analg.*, vol. 112, no. 3, pp. 678–687, Mar. 2011.
- [44] P. M. Nair, T. G. Hornby, and A. L. Behrman, "Minimal detectable change for spatial and temporal measurements of gait after incomplete spinal cord injury," *Topics Spinal Cord Inj. Rehabil.*, vol. 18, no. 3, pp. 273–281, Jul. 2012.
- [45] S. S. Sawilowsky, "New effect size rules of thumb," *J. Modern Appl. Stat. Methods*, vol. 8, no. 2, pp. 597–599, 2009.
- [46] J. Martin Bland and D. G. Altman, "Statistical methods for assessing agreement between two methods of clinical measurement," *Lancet*, vol. 327, no. 8476, pp. 307–310, Feb. 1986.
- [47] Y. Zimmermann, A. Forino, R. Riener, and M. Hutter, "ANYexo: A versatile and dynamic upper-limb rehabilitation robot," *IEEE Robot. Automat. Lett.*, vol. 4, no. 4, pp. 3649–3656, Oct. 2019.
- [48] T.-Y. Hsieh, Y.-T. Liu, and K. M. Newell, "Submovement control processes in discrete aiming as a function of space-time constraints," *PLos One*, vol. 12, no. 12, pp. 1–14, 2017, doi: 10.1371/journal.pone.0189328.
- [49] J. M. Wagner, C. E. Lang, S. A. Sahrmann, D. F. Edwards, and A. W. Dromerick, "Sensorimotor impairments and the first few months of recovery," *Phys. Ther.*, vol. 87, no. 6, pp. 751–765, 2007.